



Surface Chemistry

International Edition: DOI: 10.1002/anie.201708118
German Edition: DOI: 10.1002/ange.201708118

A Space-Charge Treatment of the Increased Concentration of Reactive Species at the Surface of a Ceria Solid Solution

Alexander F. Zurhelle, Xiaorui Tong, Andreas Klein, David S. Mebane, and Roger A. De Souza*

Abstract: A space-charge theory applicable to concentrated solid solutions (Poisson-Cahn theory) was applied to describe quantitatively as a function of temperature and oxygen partial pressure published data obtained by in situ X-ray photoelectron spectroscopy (XPS) for the concentration of Ce^{3+} (the reactive species) at the surface of the oxide catalyst $Ce_{0.8}Sm_{0.2}O_{1.9}$. In contrast to previous theoretical treatments, these calculations clearly indicate that the surface is positively charged and compensated by an attendant negative spacecharge zone. The high space-charge potential that develops at the surface (> 0.8 V) is demonstrated to be hardly detectable by XPS measurements because of the short extent of the spacecharge layer. This approach emphasizes the need to take into account defect interactions and to allow deviations from local charge neutrality when considering the surfaces of oxide catalysts.

The surface of an ionic crystal does not have to obey local charge neutrality. In fact, a charge-neutral surface is the special case. The general case, as demanded by thermodynamics, is a charged surface, with global charge neutrality being satisfied by an adjacent space-charge zone that extends many nanometers into the bulk. [1-5] Both charged surface and compensating space-charge zone will be characterized by defect concentrations that differ hugely from the bulk values, with defect concentrations at the very surface (the reaction partners of molecules in the gas phase) not necessarily being related in any simple manner to defect concentrations in the bulk phase.

Solid solutions based on cerium(IV) oxide (CeO₂, ceria), apart from being used as three-way catalysts in the treatment of automotive exhaust gas,^[6,7] are promising electrochemical catalysts for solid oxide fuel cells (SOFC) and electrolyzer cells (SOEC).^[8,9] Much recent work has focused on point-defect concentrations at ceria surfaces, and especially on their role in hydrogen oxidation and water splitting.^[9-19] The

[*] A. F. Zurhelle, Prof. Dr. R. A. De Souza Institute of Physical Chemistry, RWTH Aachen University 52074 Aachen (Germany) E-mail: desouza@pc.rwth-aachen.de

X. Tong, Prof. D. S. Mebane Department of Mechanical and Aerospace Engineering West Virginia University, Morgantown, WV 26506 (USA)

Prof. Dr. A. Klein Institute of Materials Science, TU Darmstadt 64287 Darmstadt (Germany)

Supporting information and the ORCID identification number(s) for the author(s) of this article can be found under: https://doi.org/10.1002/anie.201708118. presence of a space-charge layer has been generally ignored, however.

Chueh and co-workers have conducted extensive characterization of ceria surfaces.^[9,16,17,19] In particular they used ambient pressure X-ray photoelectron spectroscopy (AP-XPS) to determine the concentration of Ce3+ moieties at the (100) surface of Ce_{0.8}Sm_{0.2}O_{1.9} in situ at high temperatures and in reducing conditions.^[9] They found that the site fraction of Ce³⁺ at the surface is orders of magnitude higher than in the bulk and also shows a much weaker dependence on oxygen partial pressure. These two findings were interpreted in terms of the reduction enthalpy at the surface being lower than in the bulk. While this interpretation is qualitatively consistent with both findings, it does assume that the surface is charge neutral and it does not require electrochemical equilibrium for point defects between bulk and surface. In a further publication, [16] Chueh and colleagues conclude that the surface space-charge zone is negligible, that is, that the surface is (close to) neutral. Their discussion of space-charge zones, however, assumes the matrix (Ce_{0.8}Sm_{0.2}O_{1.9}) to be a dilute solution: with 20% substitution of the cation sublattice, the system is clearly a concentrated solid solution. Furthermore, their experiments only probe a possible variation in the surface space-charge potential with applied electrical bias, and not the absolute value of the space-charge potential. A significant space-charge potential that showed little variation with applied potential would, therefore, be consistent with their data. Recently, Zhao et al.[18] reproduced the data of Chueh et al.^[9] by defect-chemical modeling. They included electrochemical equilibrium between surface and bulk for mobile defects, but assumed, similarly, dilute solution thermodynamics for a concentrated solid solution and restricted the treatment to the charge-neutral case.

Herein, we apply Poisson–Cahn theory^[4] to the experimental data reported by Chueh et al.^[9] for the (100) surface of Ce_{0.8}Sm_{0.2}O_{1.9}. Poisson–Cahn theory is a framework for describing space-charge layers at extended defects (surfaces, dislocations, grain boundaries) in concentrated solid solutions. This is accomplished by calculating activity coefficients for point-defect species in terms of local and non-local defect interactions. Our approach thus relaxes all previous constraints: it allows the surface to become charged, if necessary; it describes point-defect behavior at an extended defect in a concentrated solid solution; and it maintains electrochemical equilibrium for all mobile point defects in the system.

Space-charge theories describe how point-defect concentrations in a bulk phase are modified by the presence of an extended defect. Since Poisson–Cahn theory, as noted above, takes defect–defect interactions into account, we first consider a defect chemical model with defect interactions for the



bulk phase and we then expand this model to include the surface. In this way, the treatments of point defects in the bulk phase and at the surface have a common basis.

Three point defects are important in $Ce_{0.8}Sm_{0.2}O_{1.9}$ at T < 1000 K in reducing atmospheres. [20,21] In Kröger–Vink notation, these are: 1) Sm'_{Ce} , which are Sm cations residing on the Ce sublattice and constituting acceptor-type defects; 2) $V_O^{\bullet \bullet}$, vacancies on the oxygen sub-lattice; and 3) Ce'_{Ce} , electrons that are localized at cerium ions as small polarons, [22] corresponding formally to a change in oxidation state from Ce^{4+} to Ce^{3+} . In the bulk phase, electroneutrality stipulates that the site fractions of these defects obey Equation (1):

$$a + n = 4v \tag{1}$$

where a and n are the fractions of Ce sites occupied by Sm'_{Ce} and Ce'_{Ce} , respectively; and v denotes the fraction of oxygen sites occupied by $V_O^{\bullet\bullet}$ (the factor 4 appears because there are twice as many anion as cation sites and because oxygen vacancies are doubly charged). Although a is fixed, v and n may both vary with temperature (T) and oxygen partial pressure (pO_2) on account of the reduction of ceria [Equation (2)]:

$$2Ce_{Ce}^{x}+O_{O}^{x} \equiv 2Ce_{Ce}^{\prime}+V_{O}^{\bullet \bullet}+\frac{1}{2}O_{2} \tag{2} \label{eq:2}$$

Equation (2) indicates that, in equilibrium, the electrochemical potentials of the building units of polarons $(Ce'_{Ce}-Ce^x_{Ce})$ and oxygen vacancies $(V^{\bullet\bullet}_O-O^x_O)^{[23]}\tilde{\mu}_n$ and $\tilde{\mu}_v$ respectively, are related through Equation (3)

$$2\tilde{\mu}_{n} + \tilde{\mu}_{v} + \frac{1}{2}\mu_{O_{2}} = 0 \tag{3}$$

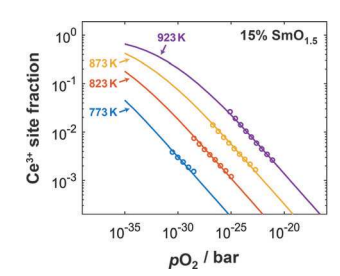
where μ_{O_2} is the chemical potential of oxygen gas $(=\mu_{O_2}^\circ + RT \ln[pO_2/p^\circ O_2])$. To include defect interactions in the description of bulk defect chemistry and bearing in mind the result for the inhomogeneous case (see Refs. [4,5] and also later), we assume pairwise interactions that are proportional to defect concentrations. Consequently, the electrochemical potential of Ce'_{Ce} as building units for the homogeneous bulk phase, $\tilde{\mu}_n$, for example, is given by Equation (4)

$$\tilde{\mu}_{\rm n} = \mu_{\rm n}^{\circ} + f_{\rm nn} n + f_{\rm an} a + f_{\rm vn} v + RT \ln \left(\frac{n}{1-a-n}\right) - F\phi \tag{4} \label{eq:munu}$$

where $\mu_{\rm n}^{\circ}$ is the standard chemical potential of ${\rm Ce'_{Ce}}$; the three subsequent terms describe the defect–defect interactions with the parameters f_{ij} as interaction energies between defects i and j; the penultimate term arises from the mixing entropy of ${\rm Ce'_{Ce}}$ on the cation sublattice; the last term, $-F\phi$, is the electrostatic contribution to the electrochemical potential, with electrostatic potential ϕ . The electrochemical potential for ${\rm V_{O}^{\bullet \bullet}}$ (building units) in the bulk phase is formulated in a similar fashion.

This model [that is, Eqs. (1), (3) and (4)] was fitted to experimentally determined site fractions of Ce³⁺ in the bulk for two different acceptor concentrations.^[9,24] As shown in Figure 1, the model describes the experimental data well at both acceptor concentrations with a single set of parameters

Angew. Chem. Int. Ed. 2017, 56, 14516-14520



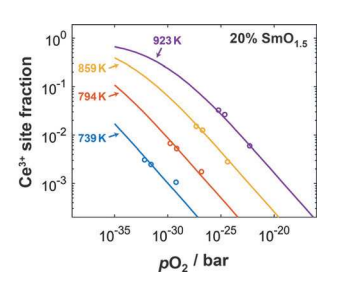


Figure 1. Bulk Ce³⁺ site fraction as a function of oxygen partial pressure for four temperatures and acceptor site fraction of 0.15 (left) and 0.20 (right). The results of the bulk model with fitted reaction and interaction parameters (solid lines) are compared with experimental data (circles) of Chueh et al.^[9,25]

(with the characteristic dependence $n \propto p O_2^{-1/4}$ also being reproduced). Without defect interactions, it is not possible to describe both datasets with one set of parameters.

Considering now the surface, we first specify why the space-charge layer forms. The sole driving energy for space-charge formation is taken to be the preferential formation of by $V_0^{\bullet\bullet}$ at the surface, $^{[25]}\Delta\mu_v^\circ=\mu_{v,\text{surf}}^\circ-\mu_{v,\text{bulk}}^\circ<0$. The potential roles of adsorbates, such as ${\rm CO_3}^{2^-}$ or ${\rm OH^-},^{[26,27]}$ in determining the space-charge potential are ignored here because their inclusion requires more experimental data than is currently available. Second, following previous work, $^{[4,5,28-30]}$ we express the electrochemical potential of ${\rm Ce'_{Ce}}$ for a one-dimensional, inhomogeneous system as Equation (5)

$$\tilde{\mu}_{n} = \mu_{n}^{\circ} + f_{nn}n(x) + f_{an}a(x) + f_{vn}v(x) + RT \ln\left(\frac{n(x)}{1 - a(x) - n(x)}\right) - F\phi - \beta_{n}\frac{\partial^{2}n}{\partial x^{2}}$$

$$(5)$$

The first six terms are identical to those for the homogeneous case [Eq. (4)], but now the site fractions of the defects and the electrostatic potential are functions of the spatial coordinate x. The seventh (last) term takes into account the gradient energy contribution to the electrochemical potential, with β_n as the gradient energy coefficient for Ce'_{Ce} . The gradient energy is an energetic penalty for concentration gradients in the system: the steeper the gradient, the larger the penalty. The electrochemical potentials for Sm'_{Ce} and $V_O^{\bullet \bullet}$ have analogous forms. In equilibrium, the electrochemical potential of a mobile defect is constant throughout the system (we discuss below which defects count as mobile). It is the combination of electrochemical potentials of the form of Equation (5) with the Poisson equation that constitutes Poisson-Cahn theory. The solution of such equations yields $\phi(x)$, n(x), and v(x) [and depending on the behavior of the dopant, a(x)]. One important benefit in using this functional form for the electrochemical potentials is that it allows other effects, such as volume changes accompanying defect formation,^[31] to be included implicitly.

At the temperatures typical for hydrogen oxidation or water splitting ($673 \le T/K \le 973$), only oxygen vacancies and polarons are sufficiently mobile to obtain electrochemical equilibrium. The acceptor cations, in contrast, are expected to become mobile only at much higher temperatures, [32] a view supported by recent modelling of cation segregation kinetics







based on Poisson-Cahn theory. [33] It is expected, therefore, that the acceptor cations are not in electrochemical equilibrium and that their site fraction a is constant throughout the sample. AP-XPS measurements, [9] however, found that a is significantly increased at the surface (0.3 instead of 0.2). It is unclear whether this increase is due to an equilibrium segregation profile generated during deposition or owing to a situation in which the acceptor cations have started to move, but have not been given sufficient time to achieve equilibrium. Because of this lack of clarity and because the inclusion of kinetic effects^[33] would greatly increase the number of parameters to be fitted, the models applied here are stationary and thus restricted to the two extreme cases: 1) the acceptors are homogeneously distributed, immobile, and thus not in electrochemical equilibrium (Mott-Schottky case: MS); 2) the acceptors are mobile and in electrochemical equilibrium (Gouy-Chapman case: GC).

Lastly, we recognise that the concentrations of Ce'_{Ce} calculated from the Poisson–Cahn models need to be convolved with the XPS attenuation function to be directly comparable with the experimentally measured data:

$$n_{\text{expt}}^{\text{surf}} = \frac{\int n(x) \exp(-x/\lambda) dx}{\int \exp(-x/\lambda) dx}$$
 (6)

In Figure 2 we compare the results for the GC case with the experimental data of Chueh et al.^[9] (Figure S1 in the Supporting Information shows the MS case).

The important result is that in both cases, a set of parameters is obtained that simultaneously describes the Ce^{3+} site fraction in the bulk and at the surface in excellent agreement with the experimentally determined data. Since the experimental XPS data of Chueh et al.^[9] can be described using $\nabla a = 0$ (MS) or $\nabla \tilde{\mu}_a = 0$ (GC), (and also with a charge neutral surface^[18]), there is evidently insufficient experimental data available to identify a unique set of parameters. All

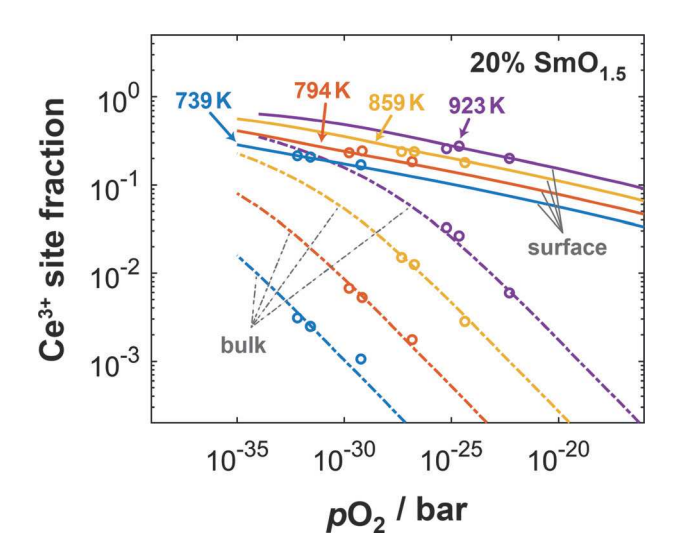


Figure 2. Surface (solid lines) and bulk (dashed lines) Ce³⁺ site fraction as a function of oxygen partial pressure for four temperatures. The calculated Ce³⁺ site fraction from the Poisson–Cahn model (lines) for the Gouy–Chapmann (GC) case are compared with experimental data (circles).^[24]

that can be said is that we have two sets of parameters that are consistent with the experimental data and that were derived without any artificial constraints. The fitted parameters are compared in the Supporting Information, Table S1 with reported data. [24,34-42] We comment on selected parameters obtained from the GC fit.

The enthalpy of the reduction reaction [Eq. (2)], $\Delta H = 4.28 \, \mathrm{eV}$, is slightly higher than reported values^[24] of 4.21 eV, but a certain difference is to be expected. We consider defect-defect interaction energies f_{ij} separately, whereas the standard literature treatment assumes a dilute solution of non-interacting defects, which results in the interaction energies being included in the value obtained.

The segregation energy of oxygen vacancies to the (100) surface (as the sole assumed driving energy for space-charge formation) was found to be $\Delta \mu_{v}^{\circ} = -1.1$ eV. This is a physically reasonable value, being the difference of two defect formation energies. No data for this surface termination are available for a direct comparison, but our value does fall comfortably into the range of values reported for other terminations: Experimental measurements on a powder by Tschöpe et al. [25] yielded $\Delta \mu_{\rm v}^{\circ} = -2.3$ eV, and atomistic calculations by Sayle et al.[34] yielded values of -1.5 eV, -2.5 eV, and -0.4 eV for the (110), (310), and (111) surfaces; the (100) surface was not examined because it has a non-zero surface dipole (Tasker Type 3 surface^[43]) and is therefore unstable without substantial reconstruction. The charging of the (100) surface due to vacancy segregation may provide the required stabilization.

Lastly, the defect–defect interaction energies for the most part are in close agreement with literature data. $^{[39,41,42]}$ Only f_{vv} shows a substantial deviation: previous investigations reported a strong repulsive interaction between oxygen vacancies (large, positive f_{vv}), whereas our fits indicate a weak attractive interaction (small, negative f_{vv}). This deviation is tentatively ascribed to other interactions that were only implicitly considered in our model, for example, volume change accompanying defect formation. $^{[31]}$

In Figure 3, charge-carrier distributions at and close to the surface are plotted exemplarily for the Gouy-Chapman case at T = 773 K and $pO_2 = 10^{-22}$ Pa. In this case, the acceptor site fraction close to the surface is constrained to the value (=0.3)determined by Chueh et al. [9] One sees that v(x) is substantially enhanced at the surface and diminished in the adjacent region, compared with the bulk value. This is due to the redistribution of oxygen vacancies from bulk to interface, driven by $\Delta \mu_{\rm v}^{\circ} < 0$. The positive charge of the vacancies at the surface is only partially compensated by increases in a(x) and n(x); the negative space-charge layer of circa 1 nm thickness is due to the lack of oxygen vacancies and also due to the accumulation of electrons. Also shown in Figure 3 is the electrostatic potential distribution. It is 0.8 V at the surface for this T and pO2, and varies, for the GC case, weakly between 0.78 to 0.88 V for the range of conditions shown in Figure 2. It is stressed that, in contrast to the dilute case [for which Boltzmann statistics holds; for example, $n(x) = n_{\text{bulk}} \exp(F\phi(x)/RT)$ and $a(x) = a_{\text{bulk}} \exp(F\phi(x)/RT)$], there is no simple relationship between point-defect concentrations at the surface and $\phi(x)$ [see Eq. (5)] and similarly





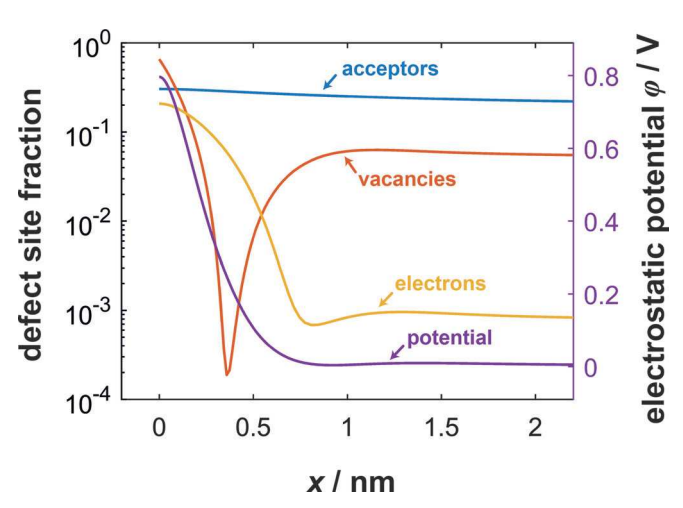


Figure 3. Defect site fractions of Sm'_{Ce} (blue), $V_0^{\bullet\bullet}$ (red) and Ce'_{Ce} (yellow), and the resulting electrostatic potential profile (violet) at the surface of $Ce_{0.8}Sm_{0.2}O_{1.9}$ calculated within Poisson–Cahn theory for the Gouy–Chapman case at T=773 K and an oxygen partial pressure of $pO_2=10^{-22}$ Pa.

charged defects may display different concentration profiles of radically different forms (compare n(x) and a(x) in Figure 3).

Finally, we turn to the issue of the measured space-charge potential. The XPS data of Feng et al. [17] indicated, for probing depths of 6 Å and 12 Å, a negligible shift in binding energies ($\leq |\pm 0.1| \, \mathrm{eV}$), and hence, because binding energies in XPS depend on the electrostatic potential, a negligible space-charge potential. Here we demonstrate that a negligible shift in XPS binding energy is entirely consistent with the calculated potential profile of Figure 3. To determine quantitatively the shift in XPS binding energy that is experimentally measurable (in the case of a surface space-charge layer whose extension is comparable with the inelastic mean free path of the photoelectrons λ), we convolve the peak shape for a constant potential $I(E_0)$ with the potential distribution $\phi(x)$ and the attenuation of the photoelectron signal [Eqaution (7)]:

$$I(E) = \int I(E_0 - \phi(x)) \exp(-x/\lambda) dx$$
 (7)

XP spectra calculated with the potential profile shown in Figure 3 and with $\lambda\!=\!6$ Å or 12 Å are shown in Figure 4. Compared with the spectrum expected for a constant potential at the bulk value, the calculated spectra are shifted slightly and are broadened asymmetrically. The slight shift in binding energies for XPS measurements with the two probing depths, importantly, is calculated to be only 0.26–0.12 = 0.14 eV. The space-charge potential of 0.8 V calculated with Poisson–Cahn theory is thus entirely consistent with published XPS data. $^{[16,17]}$

In conclusion, we have matched the progress in in situ spectroscopic studies of the surfaces of oxide catalysts by advancing the description of the physical chemistry of the surfaces. Specifically, by applying Poisson–Cahn theory to the surface of the oxide catalyst Ce_{0.8}Sm_{0.2}O_{1.9}, we have found that

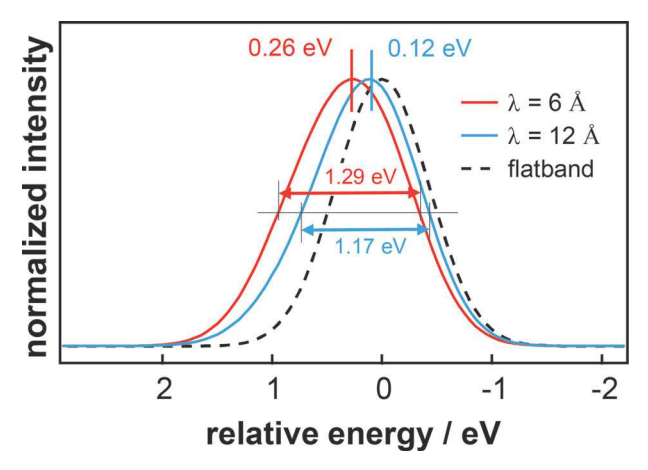


Figure 4. Photoelectron spectra calculated using Equation (7) where $I(E_0)$ is a single Gaussian line shape with a full width at half maximum of 1 eV. The dashed line refers to the potential with zero space-charge potential. The potential distribution is the same as that shown in Figure 3. The zero of the energy axis corresponds to the bulk potential.

a substantial space-charge potential develops at the surface of this concentrated solid solution, and we are able to describe reported data for the concentration of reactive surface species. Various parameters sets are found to describe the data, indicating that further experimental data on defect concentrations at and close to the surface is required. Such data would also permit the role of adsorbates in determining the chemistry of the surface to be elucidated.

Acknowledgements

The authors acknowledge funding from the Deutsche Forschungsgemeinschaft (DFG): from the collaborative research center SFB 917 "Nanoswitches"; from project SO499/7-1; and from project KL1225/7-1.

Conflict of interest

The authors declare no conflict of interest.

Keywords: ceramics \cdot ceria \cdot space—charge theory \cdot surface chemistry \cdot thermodynamics

How to cite: Angew. Chem. Int. Ed. **2017**, 56, 14516–14520 Angew. Chem. **2017**, 129, 14708–14712

- [1] J. Maier, Prog. Solid State Chem. 1995, 23, 171-263.
- [2] J. Jamnik, J. Maier, S. Pejovnik, Solid State Ionics 1995, 75, 51.
- [3] R. A. De Souza, Phys. Chem. Chem. Phys. 2009, 11, 9939 9969.
- [4] D. S. Mebane, R. A. De Souza, Energy Environ. Sci. 2015, 8, 2935–2940.
- [5] D. S. Mebane, Comput. Mater. Sci. 2015, 103, 231-236.
- [6] A. Trovarelli, Catal. Rev. Sci. Eng. 1996, 38, 439-520.
- [7] M. Ozawa, J. Alloys Compd. 1998, 275-277, 886-890.
- [8] A. Atkinson, S. Barnett, R. J. Gorte, J. T. S. Irvine, A. J. McEvoy, M. Mogensen, S. C. Singhal, J. Vohs, *Nat. Mater.* 2004, 3, 17.

Communications





- [9] W. C. Chueh, A. H. McDaniel, M. E. Grass, Y. Hao, N. Jabeen, Z. Liu, S. M. Haile, K. F. McCarty, H. Bluhm, F. El Gabaly, Chem. Mater. 2012, 24, 1876-1882.
- [10] W. C. Chueh, S. M. Haile, Philos. Trans. R. Soc. London Ser. A **2010**, 368, 3269 – 3294.
- [11] S. C. DeCaluwe, M. E. Grass, C. Zhang, F. E. Gabaly, H. Bluhm, Z. Liu, G. S. Jackson, A. H. McDaniel, K. F. McCarty, R. L. Farrow, M. A. Linne, Z. Hussain, B. W. Eichhorn, J. Phys. Chem. C 2010, 114, 19853 - 19861.
- [12] C. Zhang, M. E. Grass, A. H. McDaniel, S. C. DeCaluwe, F. El Gabaly, Z. Liu, K. F. McCarty, R. L. Farrow, M. A. Linne, Z. Hussain, G. S. Jackson, H. Bluhm, B. W. Eichhorn, Nat. Mater. **2010**, 9, 944.
- [13] W. C. Chueh, C. Yang, C. M. Garland, W. Lai, S. M. Haile, Phys. Chem. Chem. Phys. 2011, 13, 6442-6451.
- [14] D. R. Mullins, P. M. Albrecht, T. Chen, F. C. Calaza, M. D. Biegalski, H. M. Christen, S. H. Overbury, J. Phys. Chem. C **2012**, 116, 19419 – 19428.
- [15] C. Zhang, Y. Yu, M. E. Grass, C. Dejoie, W. Ding, K. Gaskell, N. Jabeen, Y. P. Hong, A. Shayorskiy, H. Bluhrn, W. X. Li, G. S. Jackson, Z. Hussain, Z. Liu, B. W. Eichhorn, J. Am. Chem. Soc. 2013, 135, 11572.
- [16] Z. A. Feng, F. El Gabaly, X. Ye, Z. Shen, W. C. Chueh, Nat. Commun. 2014, 5, 4374.
- [17] Z. A. Feng, C. Balaji Gopal, X. Ye, Z. Guan, B. Jeong, E. Crumlin, W. C. Chueh, Chem. Mater. 2016, 28, 6233-6242.
- [18] Z. Zhao, M. Uddi, N. Tsvetkov, B. Yildiz, A. F. Ghoniem, J. Phys. Chem. C 2016, 120, 16271-16289.
- [19] C. B. Gopal, F. E. Gabaly, A. H. McDaniel, W. C. Chueh, Adv. Mater. 2016, 28, 4692.
- [20] H. L. Tuller, Nonstoichiometric Oxides (Ed.: O. T. Sorensen), Academic Press, New York, 1981, p. 271 - 335.
- [21] S. Luebke, H. Wiemhoefer, Solid State Ionics 1999, 117, 229-
- [22] H. Tuller, A. Nowick, J. Phys. Chem. Solids 1977, 38, 859-867.
- [23] W. Schottky, Halbleiterprobleme IV (Ed.: W. Schottky), Vieweg, Braunschweig, 1958, p. 235.
- [24] W. C. Chueh, S. M. Haile, Phys. Chem. Chem. Phys. 2009, 11, 8144 - 8148.
- [25] A. Tschoepe, J. Electroceram. 2005, 14, 5-23.

- [26] Z. A. Feng, M. L. Machala, W. C. Chueh, Phys. Chem. Chem. Phys. 2015, 17, 12273-12281.
- [27] J. M. Polfus, T. S. Bjørheim, T. Norby, R. Bredesen, J. Mater. Chem. A 2016, 4, 7437-7444.
- [28] N. Denesyuk, J. Hansen, J. Chem. Phys. 2004, 121, 3613-3624.
- [29] R. E. Garcia, C. M. Bishop, W. C. Carter, Acta Mater. 2004, 52, 11 - 21.
- [30] J. W. Cahn, J. Chem. Phys. 1977, 66, 3667 3672.
- [31] B. W. Sheldon, V. B. Shenoy, Phys. Rev. Lett. 2011, 106, 216104.
- [32] S. Beschnitt, T. Zacherle, R. A. De Souza, J. Phys. Chem. C 2015, 119, 27307.
- [33] X. Tong, D. S. Mebane, Solid State Ionics 2017, 299, 78.
- [34] T. Sayle, S. Parker, C. Catlow, Surf. Sci. 1994, 316, 329 336.
- [35] R. Gerhardt-Anderson, A. Nowick, Solid State Ionics 1981, 5, 547 - 550.
- [36] M. Nakayama, M. Martin, Phys. Chem. Chem. Phys. 2009, 11, 3241 - 3249.
- [37] S. Bishop, K. Duncan, E. Wachsman, Acta Mater. 2009, 57, 3596-3605.
- [38] M. Nakayama, H. Ohshima, M. Nogami, M. Martin, Phys. Chem. Chem. Phys. 2012, 14, 6079 – 6084.
- [39] T. Zacherle, A. Schriever, R. A. De Souza, M. Martin, Phys. Rev. B 2013, 87, 134104.
- [40] S. Grieshammer, T. Zacherle, M. Martin, Phys. Chem. Chem. Phys. 2013, 15, 15935-15942.
- [41] S. Grieshammer, B. O. Grope, J. Koettgen, M. Martin, Phys. Chem. Chem. Phys. 2014, 16, 9974-9986.
- [42] S. Grieshammer, M. Nakayama, M. Martin, Phys. Chem. Chem. Phys. 2016, 18, 3804-3811.
- [43] P. Tasker, J. Phys. C 1979, 12, 4977.
- [44] N. Ohashi, H. Yoshikawa, Y. Yamashita, S. Ueda, J. Li, H. Okushi, K. Kobayashi, H. Haneda, Appl. Phys. Lett. 2012, 101, 251911.

Manuscript received: August 8, 2017 Revised manuscript received: September 14, 2017 Accepted manuscript online: September 18, 2017 Version of record online: October 12, 2017